

Moduli of Pavement Systems from Spectral Analysis of Surface Waves

J.S. HEISEY, K.H. STOKOE II, AND A.H. MEYER

A nondestructive technique for pavement evaluation is necessary to determine moduli of the various materials in existing pavement systems. Dynamic field testing can be used to calculate moduli from velocities of surface waves propagating through the different layers of the pavement system. A new, efficient technique incorporating an impulsive source has been developed to replace the slower, steady-state vibration technique. Frequency and phase content of the surface waves generated by the source are collected with portable spectral-analysis instrumentation. Results for field tests conducted at two flexible pavement sections yielded wave velocities measured by the spectral-analysis technique that were within 10 percent of velocities determined from cross-hole tests performed at both sites. This comparison confirms that an accurate profile of velocity versus depth (hence modulus versus depth) can be obtained by using this rapid, nondestructive spectral-analysis technique.

Pavement life is usually defined as the length of service of the pavement system before maintenance or rehabilitation is required. Estimates of remaining life as well as appropriate remedial measures are based on the elastic moduli of the various pavement materials. Elastic moduli are used to characterize the stress-strain behavior of the pavement system, which in turn is used to indicate the potential for deterioration and tensile cracking in the surface layer. Numerous methods have been developed to determine elastic moduli in pavement systems in the field. This paper presents an advance in the state of the art in the application of one of these field methods, the wave-propagation method.

There are four general methods used to evaluate elastic moduli of pavement systems (1): static deflections, steady-state dynamic deflections, impact-load response, and wave propagation. The first three methods measure deflections or displacement response of the entire pavement system caused by a static or dynamic load. Moduli are then calculated indirectly by using some form of elastic-layer theory. The major drawback of these methods is that the overall stiffness of the pavement system is measured, and it is generally difficult to separate properties of the individual layers.

Wave-propagation methods measure the velocities of elastic waves traveling through the pavement system rather than the deflections caused by the vibration source. Elastic waves can be generated by steady-state vibrations or transient impulses, and they can propagate through individual layers or the entire pavement system. Wave-propagation methods offer the most direct approach to determining elastic moduli of pavement systems since each layer is uniquely identified by the wave propagation velocity of the material within the layer.

MEASUREMENT OF ELASTIC PROPERTIES BY WAVE PROPAGATION

Since the stress-strain properties of a material govern wave-propagation velocities in that material, dynamic (or seismic) testing can be used to determine wave-propagation velocities from which moduli of elastic materials can be calculated. Furthermore, most field techniques include methods to determine thicknesses or depths of different layers on the basis of wave-propagation velocities.

Wave Propagation in Elastic Half-Space

Wave motion created by a disturbance within an infinite, homogeneous, isotropic, elastic medium ("whole

space") can be described by two kinds of waves: compression waves and shear waves. These waves are called body waves because they propagate within the body of the medium. When the elastic medium forms a half-space with a surface of infinite extent on the top, a third type of wave motion occurs. This third type of wave occurs in a zone near the surface of the half-space. The surface wave is called a Rayleigh wave, after its first investigator. Each of these three waves displays a different type of motion and travels at a different velocity.

The compression wave exhibits a push-pull motion and hence is referred to as a dilatational wave. This dilatational motion occurs in the same direction as the direction of wave propagation. The compression wave travels with a faster velocity than either the shear wave or the Rayleigh wave. Since the compression wave appears first in a travel-time record of wave motions, it is commonly called the primary wave, or P-wave. The velocity of the P-wave is given by the following equation:

$$v_p = [(\lambda + 2G)/\rho]^{1/2} \quad (1)$$

where

$$\lambda \text{ (Lame's constant)} = \nu E / [(1 + \nu)(1 - 2\nu)] \quad (2)$$

$$G \text{ (shear modulus)} = E / 2(1 + \nu) \quad (3)$$

and E , ν , and ρ are Young's modulus, Poisson's ratio, and mass density, respectively, of the elastic material.

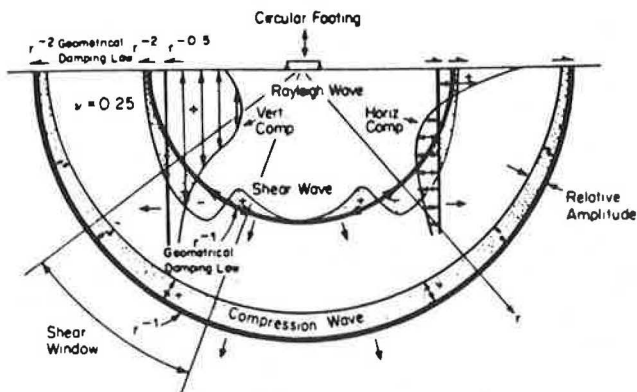
The shear wave, also called a distortional wave, exhibits shearing motion perpendicular to the direction of wave propagation. The shear wave travels significantly slower than the P-wave and, as a result, appears later in a travel-time record. It is commonly called the secondary wave, or S-wave, because it arrives after the P-wave. The velocity of the S-wave is given by the following equation:

$$v_s = (G/\rho)^{1/2} \quad (4)$$

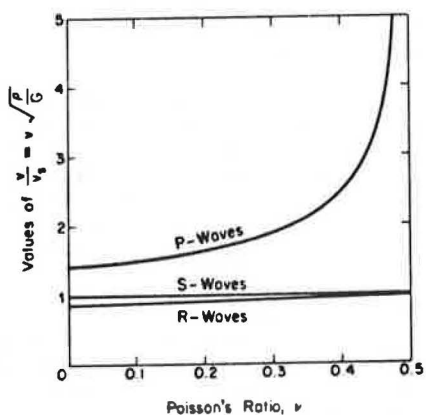
Unlike P-waves, the velocity of which can vary with the degree of saturation of a porous medium (such as soil), S-waves have the same velocity in a saturated medium as in an unsaturated medium because the fluid cannot transmit shearing motion.

The Rayleigh wave, or R-wave, does not propagate into the body of the elastic medium but travels along the surface of the half-space. The wave motion causes both horizontal and vertical particle displacements, which describe a retrograde ellipse at the surface. The amplitude of the wave decays quickly with depth so that at a depth of one wavelength, the amplitude of particle motion is only about 30 percent of the original amplitude of the surface. The velocity of the R-wave is nearly equal to the S-wave velocity, particularly for values of Poisson's ratio above about 0.25. In addition, R-wave velocity is independent of frequency in a homogeneous half-space. Since an ideal elastic half-space has a unique R-wave velocity, each frequency has a corresponding wavelength according to the following relationship:

Figure 1. Types of waves in elastic half-space.



(a) Distribution of waves from a vertically vibrating footing on a homogeneous, isotropic, elastic half-space (3).



(b) Relationship between Poisson's ratio and wave velocities in an elastic half-space (3).

$$v_R = f \cdot L_R \tag{5}$$

where f is the input frequency of excitation that generates a Rayleigh wave of wavelength L_R . The frequency-independent nature of the R-wave is the basis for certain types of dynamic testing.

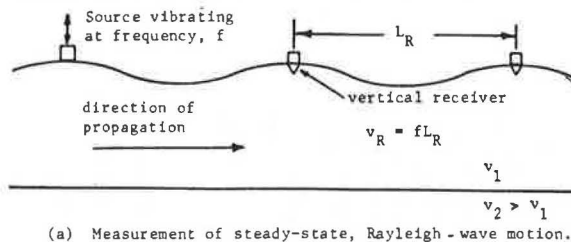
The propagation of wave energy away from a vertically vibrating circular footing at the surface of an elastic half-space is shown in Figure 1a, which illustrates the three types of waves just discussed. Miller and Pursey (2) found that 67 percent of the input energy from a vertically oscillating circular source propagated away in the form of Rayleigh wave energy, whereas 26 percent was carried by the shear wave and 7 percent was carried by the compression wave. Body waves, P- and S-waves, propagate radially outward along a cylindrical wave front at the surface. The relationships governing the geometrical damping of the wave energy as a function of radial distance from the source (r) are also shown in Figure 1a. At the surface, the P-wave and S-wave decrease in amplitude by $1/r^2$, whereas the R-wave decreases by $1/r$.

The propagation velocities of all these waves relative to the shear-wave velocity are shown as a function of Poisson's ratio in Figure 1b. Note that the velocities v_p , v_s , and v_r are the propagation velocities of the respective wave fronts and not the particle velocities of the medium itself due to the wave energy.

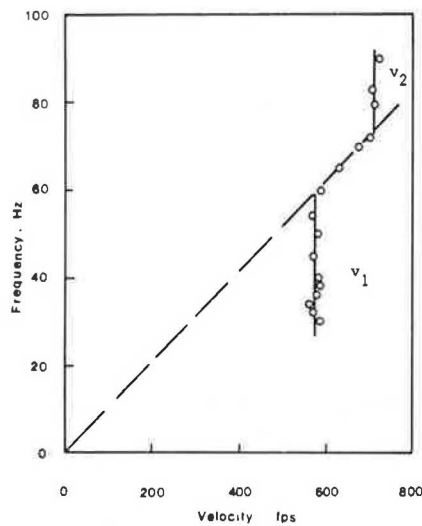
Body Waves in Layered System

In the case of a pavement system, seismic waves pro-

Figure 2. Steady-state Rayleigh-wave testing in layered systems.



(a) Measurement of steady-state, Rayleigh-wave motion.



(b) Typical results.

pagate through a layered system, which complicates the problem, especially for body waves. When body waves reach an interface between two layers, some of the body-wave energy is reflected back into the first layer and some is transmitted by refraction into the second layer. The combination of reflected and refracted body waves from a layered system greatly increases the complexity in analyzing wave arrivals, especially for measurements made at the pavement surface. In addition, pavement systems include the complication of having higher-velocity material overlying lower-velocity material (3).

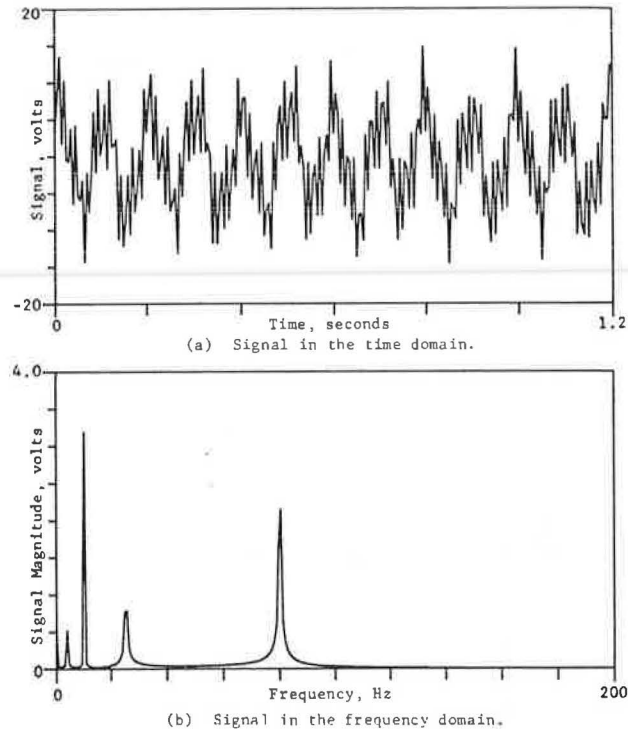
Field Techniques for Determining Wave Velocities

Various techniques are used for in situ measurement of wave velocities. The type of wave that is generated and recorded depends on the source of vibration as well as the location of receivers. Site conditions may also govern which technique is most effective.

Steady-state techniques generally use a vertically oscillating mass placed on the surface to excite the system with primarily Rayleigh waves. Vertical motion transducers are then moved along the surface until the distance between successive troughs or peaks of wave motion is established. This distance is the wavelength of the Rayleigh wave L_R , and if the frequency of vibration of the source is known, the velocity is readily determined from $v_R = f \cdot L_R$. This technique is illustrated in Figure 2. It should be noted that a range of frequencies must be excited to develop a site profile adequately.

When the steady-state technique shown in Figure 2 is used at a given site, low frequencies generate long wavelengths corresponding to deep sampling of the site. Conversely, high frequencies generate

Figure 3. Representation of complex time signal by its frequency spectrum.



short wavelengths corresponding to shallow sampling. In multilayered systems, the Rayleigh wave propagates at a velocity that reflects the material properties of the layer(s) that the wavelength samples. Short wavelengths within the surface layer will measure properties in that layer only. Long wavelengths (relative to the depth of the surface and base courses) will travel predominantly through the subgrade. Intermediate wavelengths will sample the base course or average the properties of all three materials: surface, base, and subgrade. Each wavelength will then have a corresponding phase velocity, depending on how much of each layer the wave samples.

The mathematical analysis required to interpret the relationship between phase velocity and wavelength for several typical pavement sections was studied by Jones (4). Jones assumed homogeneous elastic layers while treating the subgrade as a semiinfinite medium and showed that at infinitely long wavelengths, the phase velocity approached the R-wave velocity of the semiinfinite medium. Similarly, at very short wavelengths, the phase velocity approached the R-wave velocity of the surface layer. Theoretical solutions for an intermediate layer required more assumptions.

Although earth materials are neither perfectly homogeneous or elastic, field investigations indicate that such assumptions are reasonable. Heukelom and Foster (5) reported a profile of velocity versus depth that showed good correlation with the pavement profile when the effective sampling depth was taken as one-half of the Rayleigh wavelength. Szendrei and Freeme (6) found a similar correlation by using an effective sampling depth of approximately one-third of the Rayleigh wavelength.

Other surface measurement techniques utilize an impulsive source. Usually, velocities of P-waves are determined in these surveys. Travel times and travel distances to the received may be determined from the direct arrival or for an initial reflection in the upper layer. However, refracted waves are

normally encountered and care must be taken not to identify refracted waves as direct waves. To overcome this problem, refraction surveys are performed that take advantage of the faster-traveling refracted waves to develop the profile and corresponding velocities for a layered system. Such an analysis is greatly complicated for a site with many layers or dipping strata. Refraction surveys are also hindered when a higher-velocity layer overlies a lower-velocity layer, as in the case of a pavement surface that overlies a base course or subgrade.

An alternative to surface measurement techniques is crosshole testing (7). The source and receivers are placed in drilled holes so that direct arrivals of waves can be determined. Both P- and S-wave velocities can be measured in this type of test. Layering and velocities are accurately determined. Proper spacing of the boreholes eliminates or minimizes problems caused by refracted waves. The constraint of a quick, nondestructive test precludes this method from application in pavement evaluation. However, crosshole testing was used in this research as a tool to verify the accuracy of the proposed procedure.

Of the various wave-propagation methods, the steady-state technique appears to be most feasible for pavement testing. Unfortunately, the time required to develop the velocity profile at a given location is prohibitive. Data acquisition at just one test location may take up to several hours depending on the type of equipment used, the degree of resolution required, and the experience of the field personnel. However, if a wide range of frequencies (or wavelengths) could be excited and measured with a single excitation, the testing time could be greatly reduced. Such a procedure requires the spectral analysis of a wave pulse generated by an impact at the pavement surface.

FREQUENCY DOMAIN MEASUREMENTS

In the past 10-15 years, the development of microprocessors and the fast-Fourier-transform (FFT) algorithm has greatly extended the capability to measure and analyze dynamic systems in the frequency domain. Instrumentation now exists that rapidly filters and converts an analog signal to a digitized signal, transforms the signal from its representation in the time domain into its frequency components, and analyzes the data in various formats. Consequently, frequency spectrum analysis provides a quick and feasible approach to evaluate the propagation of elastic waves through layered systems.

Advantages of Spectral Analysis

The primary reason for utilizing spectral analysis is that information can be extracted from the data that was not apparent from the time domain representation of the signal. For example, the components of the signal in Figure 3a are indistinguishable in the time record, but each wave and its relative contribution to the overall waveform are easily observed in the frequency spectrum shown in Figure 3b. The amplitude and phase of each frequency component in the waveform can be determined. In addition, relationships between two signals can be easily identified.

Measurements in Frequency Domain

Several types of measurements can be made directly with most of the spectral analyzers that are currently available. The basic requirement is the linear spectrum, generally of both an "input" signal and an "output" signal. Other functions are defined

by using these two spectra or their complex conjugates.

The linear spectrum, denoted by $S_x(f)$, is simply the Fourier transform of the signal. The linear spectrum provides both magnitude and absolute phase information for all frequencies within the bandwidth for which the measurement was taken. Since the absolute phase is measured, a trigger is required to synchronize the signal for averaging. Linear spectrum averaging is useful for determining predominant frequencies of excitation, identifying fundamental modes and harmonics of a dynamic system, or extracting a true signal out of background noise.

The autospectral density function $G_{xx}(f)$, commonly called the autospectrum, is defined as the linear spectrum $S_x(f)$ multiplied by its own complex conjugate $S_x^*(f)$. The magnitude of the autospectrum is the magnitude squared of the linear spectrum. This magnitude can be thought of as the power (or energy of a transient impulse signal) at each frequency in the measurement bandwidth. However, multiplication by the complex conjugate eliminates the imaginary components of the spectrum, so no phase information is provided by the autospectrum. The advantage of the autospectrum is that it provides information similar to that of the linear spectrum but does not require a trigger to synchronize the averaging of signals.

The cross spectral density function $G_{yx}(f)$, or cross spectrum, is the Fourier transform of the cross-correlation function between two different signals $x(t)$ and $y(t)$. The cross spectrum is defined by the following equation:

$$G_{yx}(f) = S_y(f) \cdot S_x^*(f) \quad (6)$$

where $S_y(f)$ is the linear spectrum of the output and $S_x^*(f)$ is the complex conjugate of the linear spectrum of the input. The magnitude of $G_{yx}(f)$ is a measure of the mutual power between the two signals, making the cross spectrum an excellent means of identifying predominant frequencies that are present in both the input and output signals. The phase of $G_{yx}(f)$ is the relative phase between the signals at each frequency in the measurement bandwidth. Since the phase is a relative phase, the cross-spectrum measurement can be made without a synchronizing trigger. The cross spectrum is used primarily to determine the phase relationships between two signals that may be caused by time delays, propagation delays, or varying wave paths between receivers.

The transfer function $H(f)$, or frequency response function, characterizes the input-output relationship of a dynamic system. The frequency response function is the ratio of the spectrum of the system's response (output) to the spectrum of the system's excitation (input). Thus, the transfer function is similar to the cross spectrum. Both provide the same phase information; the magnitude of the transfer function is normalized by the autospectrum of the input $G_{xx}(f)$ relative to the magnitude of the cross spectrum. Consequently, the transfer function of a given system should be constant regardless of the input (if the system does not undergo nonlinear behavior). Generally, the input is a force measurement derived from the signal of a load cell mounted on the source of excitation. Depending on the quantity measured as output, the transfer function may provide a measurement of impedance, dynamic stiffness, or one of several other system properties. The transfer function is frequently used to identify natural frequencies and damping coefficients of a dynamic system.

The coherence function $\gamma^2(f)$ is a measurement made in conjunction with the transfer function. The

coherence is a real-valued function that is the ratio of the response (output) power caused by the measured input to the total measured response power. Therefore, if $\gamma^2(f) = 1$, all the output at the particular frequency of interest is due to the measured inputs. Reasons why the coherence function may be less than unity are as follows:

1. There are multiple input signals in the system that are not being measured;
2. Background noise is present in the measurement;
3. The frequency response function is nonlinear for the system;
4. There are closely spaced resonant peaks that cannot be detected with the given frequency resolution inherent in the digitization of the signal; or
5. Waves in the frequency range of poor coherence are not adequately excited.

EXPERIMENTAL PROCEDURE

Equipment

Two different sources were used to propagate waves through the pavement system. Each source generated an impulsive load on the surface of the pavement. Therefore, all signals were transient events. To develop a quick and efficient technique to determine the velocity profile, a wide range of frequencies (and corresponding wavelengths) must be excited by the source. An impulsive source is quicker and more efficient than a steady-state oscillator with regard to this requirement. An impact hammer is a satisfactory source if it adequately excites the bandwidth of frequencies needed to sample the pavement profile properly.

The larger source was a falling-weight deflectometer (FWD) similar to the Phoenix falling-weight deflectometer manufactured in Denmark (8). This device was mounted on a two-wheel trailer that could be towed on the highway by a passenger vehicle. The hammer was a falling mass that weighed 331 lb and could be dropped from various heights. Measurements were triggered internally by using the signal from the receiver closest to the source.

A second source, called simply a drop hammer, consisted of a cylindrical steel mass weighing approximately 6 lb. The cylinder had a hole through the center so that it could fall from any height along the 24-in rod that guided the hammer to hit the base plate, which was 2.5 in in diameter. Measurements were triggered with a resistance-capacitance (RC) trigger (7). The RC trigger permits accurate determination of the direct arrival time of the wave from the source to the receiver.

Velocity transducers, commonly called geophones, were used to detect wave propagation through the pavement system. Both vertical and horizontal geophones were employed to allow sensitivity for several different types of waves and directions of motion. The geophones were mounted on steel blocks (with a largest dimension of 2.75 in), which were then epoxied to the asphalt surface to ensure adequate coupling. The geophones had natural frequencies of 8 and 14 Hz (1 Hz = 1 cycle/s) with an approximately linear response over the range of 20-1600 Hz. Since only wave-propagation velocities (and not particle velocities) were desired, no calibration factor was determined to relate voltage to absolute particle velocity.

The instrument used to record the signals was the Hewlett-Packard Model 5420A digital signal analyzer. The instrument includes a set of signal filters, an analog-to-digital converter (ADC), a dual-channel digital oscilloscope, and a magnetic cassette tape

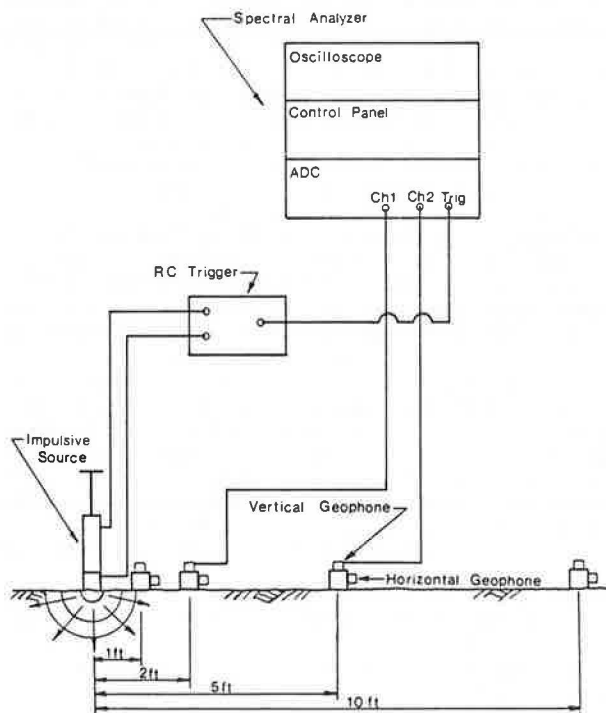
for storage and recall of permanent records. The analyzer can directly measure the frequency domain measurements previously discussed. In addition, the type of signal, type and number of averages, bandwidth (or time length), and trigger conditions can all be specified by the operator. The analyzer can be easily interfaced with an x-y plotter to provide a hard copy of the data.

Setup

The general configuration of the source, geophones, and recording equipment used in these tests is shown in Figure 4. The geophones were placed in a linear array to minimize anisotropic effects that might influence wave propagation. The line of geophones extended parallel to the direction of the roadway. Vertical geophones (subsequently identified by the symbol V) were located approximately 1, 2, 5, and 10 ft from the source. Horizontal geophones (subsequently identified by the symbol H) were located at the same positions and were aligned radially from the source so as to detect wave motion occurring in the direction of wave propagation. Hereafter, measurements are identified by the type of geophone used (V or H) and the location of the geophone(s) from the source (1, 2, 5, or 10 ft). For example, measurement V2-V5 used vertical geophones located 2 ft and 5 ft from the source.

Measurements were made by using only two geophones for any one impulse, since the recording instrument was a dual-channel device. Comparative records were taken for responses of both vertical and horizontal geophones. Both time-domain and frequency-domain measurements were recorded, although the thrust of the data acquisition was toward spectral analysis. Frequency-domain measurements included the linear spectrum, autospectrum, cross spectrum, transfer function, and coherence function. Records with one average and with five averages were used to compare the advantages of averaging.

Figure 4. Experimental setup.



Method of Analysis

Since more than two-thirds of the energy generated by a vertical force propagates away from the source in the form of a Rayleigh wave, it was assumed that the recorded responses of the geophones represented primarily R-wave motion. Analysis by using the R-wave is desirable since it is not significantly affected by reflections that complicate P-wave and S-wave analyses. Furthermore, due to the relationship between frequency and wavelength of the R-wave, the entire profile (to a depth of interest for a pavement system) can be investigated without borings being required.

By using the phase information provided by the cross spectrum, travel times can be calculated for each frequency that is excited. The phase difference θ between the signals of the input and output geophones represents the time lag or travel time Δt for an R-wave (of frequency f and velocity v_R) to propagate over the distance between the two geophones. The phase difference is 360 degrees for a travel time equal to the period of the wave T . With $T/360$ degrees as a proportionality factor, the relationship for travel time is as follows:

$$t = (T/360^\circ) \cdot \theta \quad (7)$$

Because the frequency is the inverse of the period, travel time can be written as follows:

$$t = [(\theta/360^\circ)] \cdot [(1/f)] \quad (8)$$

The distance between the geophones is a known parameter, and therefore the velocity is readily calculated by the following equation:

$$v_R = (\text{distance}/\Delta t) \quad (9)$$

Now both frequency and velocity are known, so the wavelength of the R-wave can be calculated from Equation 5. The profile of velocity versus depth is based on an appropriate fraction of the wavelengths corresponding on the effective sampling depth of the wave.

A typical set of calculations is shown in Table 1. Further details regarding the reduction and analysis of the data may be found in the report for this study (9).

Test Sites

Field tests were conducted at two sites; both profiles consisted of a subgrade, base course, and flexible pavement. Crosshole test data were available for comparison purposes at both sites.

The first site was an asphalt section of Interstate 35 in Austin, Texas (referred to here as the Austin site). The longitudinal section profile is shown in Figure 5a. The thickness of the asphalt is approximately 6.5 in. The flexible base is compacted in three layers, each approximately 5 in thick, and is underlain by a sandy subbase approximately 1 ft thick. The subgrade is primarily a stiff silty clay extending to a depth of about 13 ft. Average unit weights of the materials are 145, 140, 135, and 115 pcf for the pavement, base, subbase, and subgrade, respectively. Poisson's ratios were assumed to be 0.35 for the pavement and 0.40 for the base, subbase, and subgrade.

The second site was a section of Texas Route FM 971 near Granger (referred to here as the Granger site). The section is located on a constructed fill embankment. The subgrade is a compacted clay to a depth of approximately 20 ft. The base course is approximately 11 in thick and consists of two layers

Figure 5. Longitudinal section profiles and material properties at test sites.

Depth (ft)	Description of Material	Assumed Poisson's Ratio	Assumed Unit Weight (pcf)
0.54	Asphalt layer: 2 1/4-in. HDMAC & 4-in. ASTB	0.35	145
1.79	Flexible (crushed limestone) base placed in (3) 5-in. lifts	0.40	140
3	Subbase: dense sand with some gravel. approx. thickness = 12 - 15 in	0.40	135
6	Black, stiff clay	0.40	115
10	Tan, silty clay	0.40	115
10	Water Table		
13	Weathered Caliche limestone at approx. 12.5 - 13 ft		

(a) Austin (IH-35) site.

Depth (ft)	Description of Material	Assumed Poisson's Ratio	Assumed Unit Weight (pcf)
0.085	Two-course surface treatment	0.30	145
1.0	Flexible base (total of 11 in.)	0.35	140
	6-in. Lime-stabilized subgrade	0.40	125
	Compacted fill: stiff, tan clay (Taylor Marl)	0.45	125
10	Compacted fill: stiff, tan and black clay (mixed)	0.45	125
12	Compacted fill: stiff, black clay (Gumbo clay)	0.45	125
19	Natural soil: firm, black clay (Gumbo Clay)		

(b) Granger (FM 971) site.

Table 1. Calculations from phase of cross spectrum for determining profile of velocity versus depth.

Frequency (Hz 000s)	Phase (deg)	Travel Time (ms)	Velocity (ft/s)	Wavelength (ft)	Depth L/3 (ft)
12	18.35	4.248	1907.9	158 992	52 997
14	16.57	3.288	2465.0	176 071	58 690
16	17.17	2.981	2718.7	169 919	56 640
18	24.98	3.855	2102.3	116 793	38 931
20	34.31	4.765	1700.7	85 034	28 345
22	50.11	6.327	1280.9	58 222	19 407
24	81.28	9.407	861.5	35 894	11 965
26	109.30	11.677	694.0	26 693	8 898
28	130.89	12.985	624.1	22 290	7 430
30	149.44	13.837	585.7	19 523	6 508
32	164.78	14.304	566.6	17 705	5 902
34	175.84	14.366	564.1	16 592	5 531
36	179.80	13.873	584.1	16 226	5 409
38	187.92	13.737	590.0	15 525	5 175
40	198.78	13.804	587.1	14 677	4 892
45	228.95	14.133	573.4	12 743	4 248
50	248.71	13.817	586.5	11 731	3 910
54	275.96	14.195	570.9	10 572	3 524
59	293.72	13.655	593.5	9 933	3 311
65	300.91	12.859	630.2	9 696	3 232
69	300.18	11.998	675.5	9 719	3 240
75	310.71	11.508	704.2	9 390	3 130
79	323.33	11.369	712.8	9 023	3 008
83	343.29	11.489	705.4	8 499	2 833
90	361.33	11.152	726.7	8 074	2 691
95	374.94	10.963	739.2	7 781	2 594
100	388.62	10.795	750.7	7 507	2 502

Note: Distance between geophones = 8.104 ft.

of crushed limestone. The pavement is a two-course oil and stone surface treatment, approximately 0.5-1 in thick. The section profile is shown in Figure 5b. Unit weights of the materials were assumed to be 145, 140, and 125 pcf for the pavement, base, and subgrade, respectively. Poisson's ratios were assumed to be 0.30, 0.35, and 0.45 for the pavement, base, and subgrade, respectively.

TEST RESULTS

Austin Site

Testing was first performed by using the FWD as the source. The complete time history of the FWD is shown in Figure 6a. The signal was recorded with a geophone attached to the base of the FWD. The signal was triggered (t = 0) with the initial downward hit of the weight. A pretrigger delay was used to capture the negative-time part of the signal. The small upward displacement at approximately t = -0.25 s is due to the slight rebound of the base plate when the weight is released to undergo free fall. Multiple impacts occur for about eight or nine rebounds of the weight. These additional impacts do not interfere with the initial pavement response because all data are collected from the first impulse before the subsequent impulses occur. The time interval for a wave traveling from 2 to 10 ft is of the order of 10 ms, whereas the time interval between the first and second impacts of the weight is approximately 450 ms.

The Fourier transform of the time signal, the linear spectrum, is shown in Figure 6b. The major frequency component excited by the falling weight is approximately 21 Hz. This corresponds quite closely to the pulse created by the first trough of the signal in the time domain. This pulse width is approximately 25 ms, yielding a predominant period $T = 50$ ms or a predominant frequency of 20 Hz. The level of excitation greatly decreases with increasing frequencies.

Figure 6. Impulsive loading created by FWD.

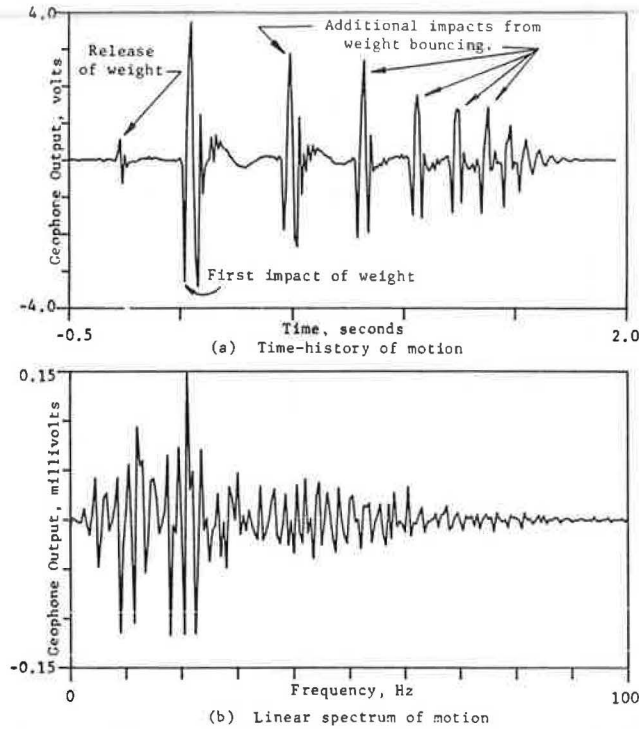
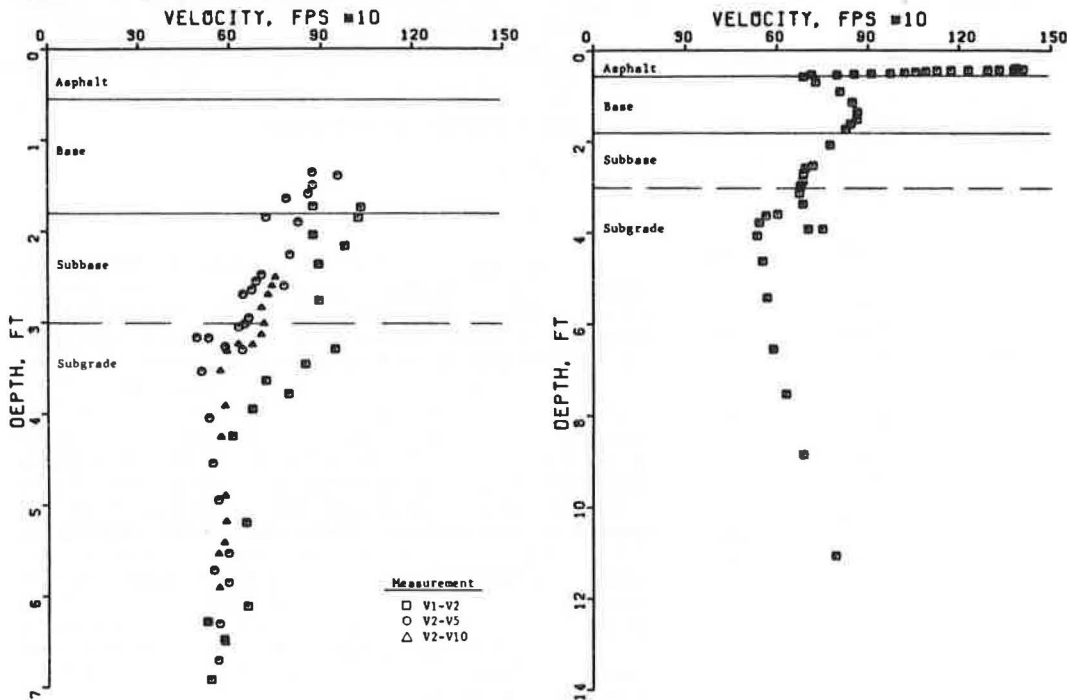


Figure 8. Rayleigh wave velocity profile: Austin site.



(a) FWD as source.

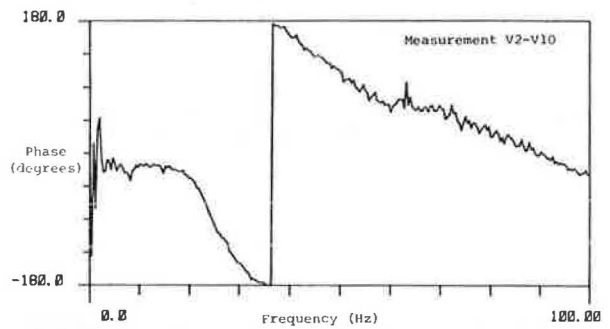
(b) Drop hammer as source.

Comparisons for both time- and frequency-domain measurements indicate that there are no significant differences between one-average records and five-average records. This is probably a result of the high reproducibility of the impulse. Occasionally, one-average records exhibited apparent anomalies. To avoid anomalies, all analyses were performed by using five-average records.

A comparison of responses from vertical geophones and horizontal geophones indicates that responses are similar, although the magnitude of the vertical response is approximately 100 times the magnitude of the horizontal response since the source is designed to input energy in the vertical direction. However, velocities obtained from measurements by using horizontal geophones were somewhat higher than those obtained from measurements by using vertical geophones. One possible explanation of this difference in velocities may be the greater sensitivity of the horizontal geophones to higher-velocity P-wave energy.

The velocity profile was determined from three records by using phase information of the cross spectrum obtained from plots such as the one in Figure 7. The three records include V1-V2 with bandwidth (BW) = 200 Hz; V2-V5 with BW = 1600 Hz

Figure 7. Plot of cross-spectrum phase versus frequency used to determine Rayleigh wave velocity.



(although useful data did not exist beyond about 250 Hz); and V2-V10 with BW = 100 Hz. A typical set of calculations is shown in Table 1. Depths given in the table were calculated by using the one-third wavelength criterion. The resulting profile is shown in Figure 8a.

Velocities could not be determined with the FWD as the source for the upper 15 in of the profile. For typical velocities of pavement materials, the FWD cannot excite high enough frequencies to generate the short wavelengths needed to sample the upper layers. Previously, it had been shown that the level of excitation of the FWD decreased with increasing frequency. Nearly all the energy of excitation is contained within 100 Hz, and essentially no frequencies are excited above 250 Hz. Above 250 Hz, the phase of the cross spectrum becomes erratic, as illustrated in Figure 9a. Similarly, the coherence displays irregularities above 250 Hz. These results indicate that the FWD does not sufficiently excite the necessary frequencies to evaluate the entire pavement system by the spectral analysis of propagated waves.

Measurements for the drop hammer source were made by using one set of vertical receivers, V2-V5. The phase of the cross spectrum, shown in Figure 9b, provides useful data up to about 1400 Hz. Concurrently, the measurement exhibits high coherence up to approximately 1300-1400 Hz.

The profile of velocity versus depth is shown in

Figure 8b. The layering in the velocity profile (which used one-third of the Rayleigh wavelength as the depth) correlates well with the actual profile. By using the profile, Rayleigh wave velocities were estimated as 1400, 860, 690, and 560 ft/s for the asphalt, base, subbase, and subgrade, respectively.

Velocities obtained from cross-spectrum measurements by using both the FWD and the drop hammer are compared in Figure 10. The profiles from the two sources agree quite closely. The R-wave velocities for each layer are summarized in Table 2. The close agreement of velocities from the relatively light load (drop hammer) with those from the relatively heavy load (FWD) suggests that the moduli of the pavement materials are not stress (strain) sensitive over the range of stresses up to and including those generated by the FWD. Consequently, a lighter and sharper impulse is more desirable to sample all materials in the pavement since the heavier FWD could not generate high enough frequencies to sample the surface layer.

Velocities from cross-spectrum (surface) measurements were also compared with velocities from cross-hole tests performed at the Austin site. Two borings were made and crosshole data were obtained for shear waves traveling directly in each layer. The S-wave velocity profile from crosshole testing,

Figure 9. Comparison of phase of cross spectrum for measurement V2-V5 by using different sources.

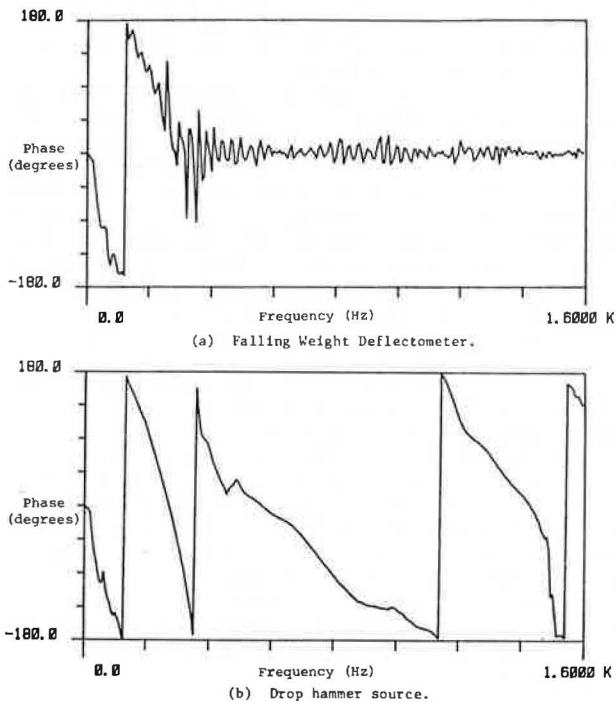


Figure 10. Comparison of crosshole velocities with shear-wave velocity profile obtained by using cross-spectrum (surface) measurements.

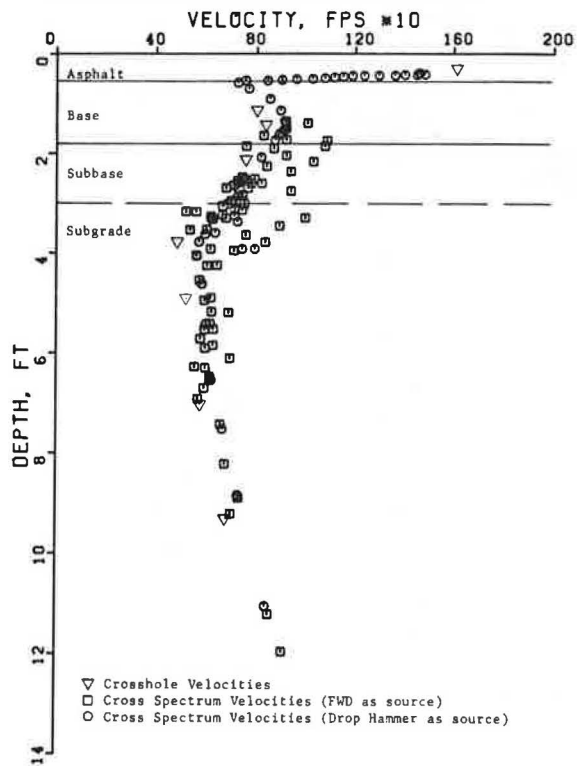


Table 2. Summary of R-wave velocities determined from cross-spectrum measurements at Austin site.

Material	Approximate Thickness (in)	Unit Weight (pcf)	Poisson's Ratio	Velocity (ft/s)			
				R-Wave			
				FWD	Drop Hammer	Avg	S-Wave
Asphalt	6.5	145	0.35	-	1400	1400	1500
Base	15	140	0.40	880	860	870	925
Subbase	12-15	135	0.40	700	690	695	740
Subgrade	120	115	0.40	580	560	570	605

shown in Figure 10, compares very closely with the S-wave velocity profiles obtained by cross-spectrum measurements. The comparison for each layer is summarized below. The close agreement in velocities with an independent technique such as crosshole testing indicates the validity and accuracy of determining velocities (moduli) from spectral analysis of surface waves by the cross-spectrum method.

Material	S-Wave Velocity (ft/s)		Percentage of Difference
	Cross-Spectrum Measurements	Crosshole Tests	
Asphalt	1500	1610	6.8
Base	925	823	12.4
Subbase	740	743	0.4
Subgrade	605	565	7.1

By using the S-wave velocities determined from cross-spectrum measurements (Table 2), a shear modulus and Young's modulus were calculated for each layer. In addition, Young's moduli for the various layers were backcalculated from deflection basins measured during Dynaflect testing conducted at the Austin site. The Young's moduli by wave propagation (cross spectrum) and those by deflection methods (Dynaflect basin) are summarized below. For the most part, the moduli determined from the two

methods are comparable, which suggests again that the cross-spectrum method is a valid and accurate approach. Slight differences in each layer may be a result of the uncertainty and variability in determining moduli by backfitting a deflection basin by using elastic theory (ELSYM5):

Material	Shear Modulus (psi 000s)	Young's Modulus E (psi 000s)	
		Wave Propagation	Deflection Method
Asphalt	70	190	250
Base	26	72	108
Subbase	16	45	40
Subgrade	9	25	17

Granger Site

Cross-spectrum measurements at the Granger section were obtained by using only the drop hammer as the source. Measurements were made along the centerline of the road and along a wheel path for various spacings of geophone pairs, ranging from 0.5 and 1 ft to 8 and 15 ft. The frequency bandwidth of the measurements was varied from 50 to 3200 Hz to obtain data for wavelengths sampling each layer.

The profile of velocity versus depth is plotted in Figure 11 by using a depth criterion of $L_R/3$. The velocity profile shows distinct layering, which correlates well with the actual section profile. By using the profile, Rayleigh wave velocities were estimated as 980, 670, and 430 ft/s for the pavement, base, and subgrade, respectively. By using the unit weights and Poisson's ratios previously listed for these materials, the Rayleigh wave velocities were converted to shear-wave velocities, and values of Young's modulus were calculated to be 91 000, 42 000, and 16 000 psi for the pavement, base, and subgrade, respectively.

Young's moduli were also backcalculated from deflection basins measured during Dynaflect testing at the Granger site. These moduli are summarized in Table 3 along with those determined from wave-propagation velocities (cross-spectrum method). The best agreement between the two methods occurs in the subgrade layer, although the overall agreement is not so good as that exhibited at the Austin site. It is not clear which method is more "accurate" nor is it clear whether the use of elastic-layer theory and deflection measurements is reasonable for a thin-layered, surface-treated pavement such as the test section at the Granger site. However, the cross-spectrum method did provide a velocity profile that correlated closely with the profile layering.

Shear-wave velocities in the subgrade determined from crosshole tests ranged from 490 to 530 ft/s compared with 420-480 ft/s for velocities determined from the spectral analysis of surface waves. The lower velocities from cross-spectrum measurements may have been a result of greater moisture in the soil following a period of heavy rainfall at the site. In any case, the difference between velocities is only about 10 percent, which is quite acceptable for engineering purposes.

Figure 11. Rayleigh wave velocity profile: Granger site.

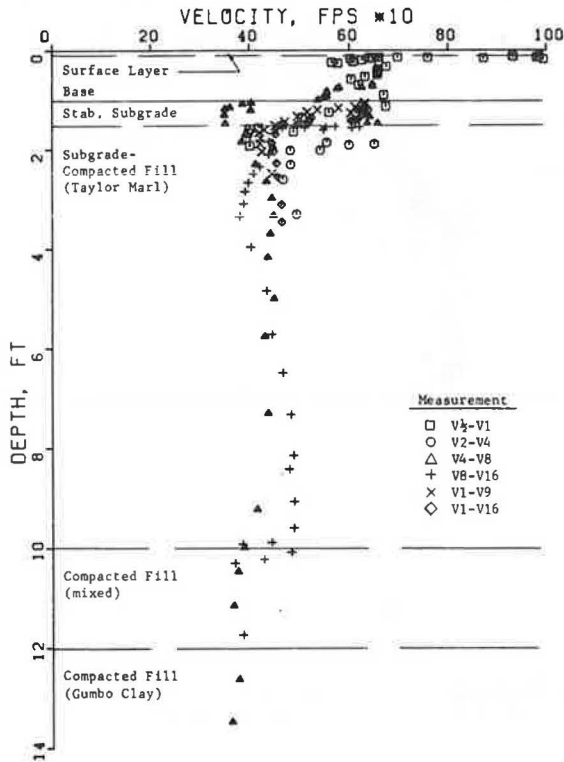


Table 3. Summary of wave velocities and elastic moduli determined at Granger site.

Material	Unit Weight (pcf)	Poisson's Ratio	Velocity (ft/s)		Shear Modulus (psi)	Young's Modulus E (psi 000s)	
			R-Wave	S-Wave		Wave Propagation	Deflection Method ^a
Surface	145	0.30	980	1060	35 000	91	50
Base	140	0.35	670	720	15 700	42	13
Stabilized subgrade	125	0.40	520	550	8 100	23	12.5
Subgrade	125	0.45	430	450	5 500	16	12

^aModuli were backcalculated from fitted deflection basin by using elastic-layer theory (ELSYM5).

SUMMARY AND CONCLUSIONS

A method to determine elastic moduli at soil and pavement sites was proposed and tested. Criteria that guided the development of this method included the restraint of nondestructive testing, accuracy of moduli for all layers regardless of thicknesses, and quickness and efficiency for rapid, extensive testing. To meet these criteria, surface receivers were utilized to evaluate the Rayleigh wave motion created by a vertical, impulsive source that could excite a wide range of frequencies with a single impact. Analysis was facilitated by using a portable spectral analyzer to study the magnitude and phase of the frequency content of the recorded wave pulse. Phase information from the cross-spectrum function was used to calculate Rayleigh wave velocities, which were converted to shear-wave velocities. Elastic moduli (shear moduli and Young's moduli) were then calculated from the shear-wave velocities.

For pavement sites consisting of a flexible (asphalt concrete) surface, frequencies up to 2-5 kHz should be excited. This upper bound will vary depending on the thickness and stiffness of the surface layer. Higher frequencies are necessary for thinner, stiffer pavements. Based on tests at two pavement sites, it appears that geophones provide good response up to at least 3 kHz. For higher frequencies, it may be necessary to use accelerometers.

Comparisons between moduli calculated from wave-propagation velocities and moduli backcalculated from measured Dynaflect deflection basins indicate that the wave-propagation method is a valid method to determine Young's modulus for each layer in a pavement system. Agreement between the two methods was quite good at the Austin site where the pavement was newly constructed but was not so good at the Granger site where the pavement was several years old and showed signs of deterioration. The poorer comparison at the Granger site may result from assumptions in the elastic-layer theory that are not reasonable for a thin, surface-treated pavement.

Shear-wave velocities in the subgrade obtained from surface measurements correlated well (typically within 10 percent) with those obtained from cross-hole testing, which suggests that the cross-spectrum (surface) method is not hindered by the relatively stiff asphalt layer at the surface. However, both of the pavement systems investigated in this study consisted of flexible surface layers, with stiffnesses about 5-10 times those for the subgrade. For rigid pavements, the stiffness of the surface layer is considerably greater and may complicate the analysis of subgrade velocities and moduli. Further research is necessary to determine whether the cross-spectrum method is applicable for rigid pavements.

Based on comparisons with shear-wave velocities from crosshole testing and Young's moduli calculated from Dynaflect deflection basins, the cross-spectrum analysis of surface waves was found to be a valid

and accurate method to determine moduli of pavement systems. Furthermore, the cross-spectrum method can be used to test a given location in only a few minutes, whereas the previous steady-state method might require several hours at a given location. As a result, the cross-spectrum method allows more data acquisition (and at lower costs) to evaluate pavement condition.

ACKNOWLEDGMENT

This research was conducted under the Cooperative Highway Research Program, Project HPR-0010(5). We are grateful for the funding support and technical services provided by the Texas State Department of Highways and Public Transportation under Research Project 3-8-80-256.

REFERENCES

1. R.L. Lytton, W.M. Moore, and J.P. Mahoney. Pavement Evaluation, Phase 1: Pavement Evaluation Equipment. FHWA, Rept. FHWA-RD-75-78, 1975
2. G.G. Miller and H. Pursey. On the Partition of Energy Between Elastic Waves in a Semi-Infinite Solid. Proceedings of the Royal Society, London, Part A, Vol. 223, 1955, pp. 251-541.
3. R.F. Richart, Jr., J.R. Hall, Jr., and R.D. Woods. Vibrations of Soils and Foundations. Prentice-Hall, Englewood Cliffs, NJ, 1970.
4. R. Jones. Surface Wave Technique for Measuring the Elastic Properties and Thicknesses of Roads: Theoretical Development. British Journal of Applied Physics, Vol. 13, 1962, pp. 21-29.
5. W. Heukelom and C.R. Foster. Dynamic Testing of Pavements. Journal of the Soil Mechanics and Foundation Division of ASCE, Vol. 86, No. SML, Feb. 1960
6. M.E. Szendrei and C.R. Freeme. Road Responses to Vibration Tests. Journal of the Soil Mechanics and Foundation Division of ASCE, Vol. 96, No. SM6, Nov. 1970, pp. 2099-2124.
7. R.J. Hoar and K.H. Stokoe II. Generation and Measurement of Shear Waves In Situ. In Dynamic Geotechnical Testing, American Society for Testing and Materials, Philadelphia, PA, Special Tech. Publ. 634, 1978.
8. A. Bohn, P. Ullidtz, R. Stubstad, and A. Sorenson. Danish Experiments with the French Falling Weight Deflectometer. Proc., 3rd International Conference on the Structural Design of Asphalt Pavements, Univ. of Michigan, Ann Arbor, Vol. 1, 1972, pp. 1119-1128.
9. J.S. Heisey. Determination of In Situ Shear Wave Velocities from Spectral Analysis of Surface Waves. Univ. of Texas at Austin, Master's thesis, 1981.